Asia Pac. J. Math. 2023 **10**:18

# IMPACT OF CORRUPTION IN A SOCIETY WITH EXPOSED HONEST INDIVIDUALS: A MATHEMATICAL MODEL

ADETAYO SAMUEL EEGUNJOBI[1,*], OLUWOLE DANIEL MAKINDE[2]

[1]Mathematics Department, Namibia University of Science and Technology, Windhoek, Namibia

[2]Faculty of Military Science, Stellenbosch University, Private Bag X2, Saldanha 7395, South Africa

[*]Corresponding author: samdet1@yahoo.com

Received Apr. 22, 2023

Abstract. This study presents a non-linear mathematical model to analyze the impact of corruption on a society where honest individuals are exposed to corrupt practices. The model considers key factors such as the level of corruption, the behavior of honest individuals, and the dynamics of corruption. We estimate the basic reproduction number of the model, accounting for constant recruitment and death-based demographic factors. The equilibria of the model have been analyzed in depth, and their stability has been comprehensively investigated and discussed. We carried out a sensitivity analysis on the proposed model in order to determine the primary parameters that are responsible for the model's basic reproduction number and conducted the bifurcation analysis. We present numerical simulations in order to highlight the outcomes of our analytical work. Our findings suggest that $\lambda$, $\rho$ and $\beta_2$ have a significant impact on the corrupted and honest compartments.

2020 Mathematics Subject Classification. 92D30.

Key words and phrases. corruption dynamics; basic reproduction number; stability analysis; sensitivity analysis; bifurcation analysis; numerical simulation.

## 1. Introduction

Corruption has been a widespread problem in societies all over the world, and it has a negative impact on economic growth, political equilibrium, and social cohesion. There has been a significant amount of research conducted on the effects of corruption; however, the influence that corruption has on the actions of honest indivuduals has received comparatively little attention. In this sense, a mathematical model can serve as a helpful instrument for the purpose of conducting an analysis of the dynamics of corruption in a society.

DOI: 10.28924/APJM/10-18

Mathematical modeling is one method that can be used to gain an understanding of corruption because it can provide insights into the dynamics of corruption as well as its impact on society and this has been employed in recent years to examine corruption's prevalence in society and find ways to combat it. The compartmental model, traditionally employed in the study of infectious diseases [1]- [4], has been adapted for investigating dynamics of compartmental corruption. [5] proposed a mathematical model for corruption that accounts for jail anti-corruption awareness and counseling. They determined the basic reproduction number and examines corruption-free and endemic equilibrium points and analysis on the basic reproduction number. Simulations match analytical findings. [6] used media coverage to model corruption spread and control.The basic reproduction number and positive, bounded model are determined. The model's corruption-free, endemic, and corrupted equilibria are examined for local and global stability. MATLAB's ode45 numerical simulations confirm the study's findings. A nonlinear deterministic model was proposed by [7] to analyze the dynamics of corruption utilizing stability theory of differential equations. The next-generation matrix method was used to calculate the basic reproduction number, and conditions for both local and global asymptotic stability of the corruption-free and endemic equilibria were established. The model showed forward bifurcation. The model was then expanded to an optimal control problem with two time-dependent controls to evaluate the impact of corruption on the human population. Using Pontryagin's maximum principle, the optimal control of corruption transmission was derived. Numerical simulations indicated that an integrated control strategy was necessary to combat corruption. Using age-appropriate sexual information and guidance/counseling, [8] proposed a mathematical model to examine moral corruption. Sexual knowledge divided the population into three groups. The next-generation matrix technique was employed to estimate the basic reproduction number in the well-posed model. A globally asymptotically stable morally corrupt-free equilibrium was established. Forward bifurcation showed that moral corruption could be eliminated. Numerical simulations revealed that an integrated control technique was best for moral corruption transmission and the article also discussed moral corruption-fighting factors.

To effectively address corruption and corrupt practices, it is essential to have a deep understanding of the corrupt process, as well as prevention and disengagement programs. Mathematical models can serve as an initial step in achieving this goal. Differential equations have been employed to describe issues in the social sciences since the work of [9], who was a trailblazer in the application of mathematical techniques. A deterministic SCHRS mathematical model and an extended stochastic model were developed by [10] to analyze corruption transmission dynamics. The models covered topics such as equilibrium points, reproduction numbers, and stabilities. Next-generation matrix method and twice Ito's differentiable formula were used to calculate basic reproduction numbers. Sensitivity analyses and numerical simulations were performed. Results suggested that the number of corrupted individuals in the community increased with the rate of interaction between corrupted and susceptible populations, and decreased with recovery through education or punishment. [11] addressed the issue of corruption on a global scale and formulated a mathematical model for its dynamics under control measures. The analysis of the model identified the existence of both corruption free equilibrium and corruption endemic equilibrium, and the effective reproduction number was calculated using the next-generation matrix method. The study concluded that mass education and religious teaching were the most effective parameters for controlling corruption, and combining both strategies yields better results in reducing corruption in a shorter time frame than using them separately. The study recommended the simultaneous application of both mass education and religious teaching to control corruption. [12] developed and evaluated an epidemiological model that incorporates an immunity clause to examine corruption. The simulation results suggested that it would be difficult to successfully combat corruption if the immunity clause remained in place. We conducted a literature review on the spread and transmission of corruption as if it were an infectious disease. We looked at the work of other scholars who have used mathematical modelling approaches to study the dynamics of corruption and some of these are as cited in references [13]- [18].

The aim of this study is to present a model for the spread of corruption, incorporating honest and corrupted compartments, using the framework of epidemiology to describe the dynamic transmission process. The remainder of this study is organized as follows: Section 2 outlines the formulation of the mathematical model. In section 3, we estimate the basic reproduction number, analysis of solution positivity and boundedness, and investigation of local and global stabilities of the corruption-free equilibrium. We conduct sensitivity and bifurcation analyses. Section 4 presents the results of numerical simulations. Finally, Section 5 provides the concluding remarks.

## 2. Model Problem

We provide a deterministic model that is comprised of five ordinary differential equations as a means of illustrating the dynamic nature of corruption through the use of a mathematical model. The framework of the model is divided into five unique compartments, each of which is meant to reflect the whole human population $N(t)$ at any given point in time (t). These compartments include susceptible individuals $(S(t))$, exposed individuals $(E(t))$, corrupted individuals $(C(t))$, honest individuals $(H(t))$, and individuals who have recovered from corruption $(R(t))$ such that

$$N(t) = S(t) + E(t) + C(t) + H(t) + R(t).$$

Susceptible individuals (S(t) are those who are not involved in corrupt activities but are vulnerable to corruption, exposed individuals (E(t), those who are exposed to corruption but who do not participate in corrupt practices, corrupt individuals (C(t)) are individuals who are involved in corrupt practises, honest individuals $(\mathrm{H(t)})$ are those who are truthful and are incapable of engaging in corrupt practices while recovered individuals $(\mathrm{R(t)})$ are individuals who stopped to do or practise corrupt activities. We assume positive recruitment rate to both susceptible and honest compartments $\Psi$ while $\pi$ is the proportion of the recruitment joining susceptible and $(1-\pi)$ is the proportion of the recruitment joinning honest. The susceptible individuals can join exposed compartment by contact rate $\beta_1$ with corrupt individuals and honest individuals can move to exposed compartment by contact rate $\beta_2$ with corrupt individuals. Here, we assume that $\beta_2 > \beta_1$. The exposed individuals can fully become corrupted individual with rate $\rho\tau$ while exposed individuals may leave to honest compartment with rate $\tau(1-\rho)$. The corrupt individuals can join the recover individuals with rate $\theta$ or go to prison with rate $\lambda$. The recovered individuals are joined to susceptible individuals and honest individuals with rate $\alpha\epsilon$ and $\alpha(1-\epsilon)$ respectively. We incorporate natural death in each of the compartments. Fig.1 below shows the transmission dynamics of the model.

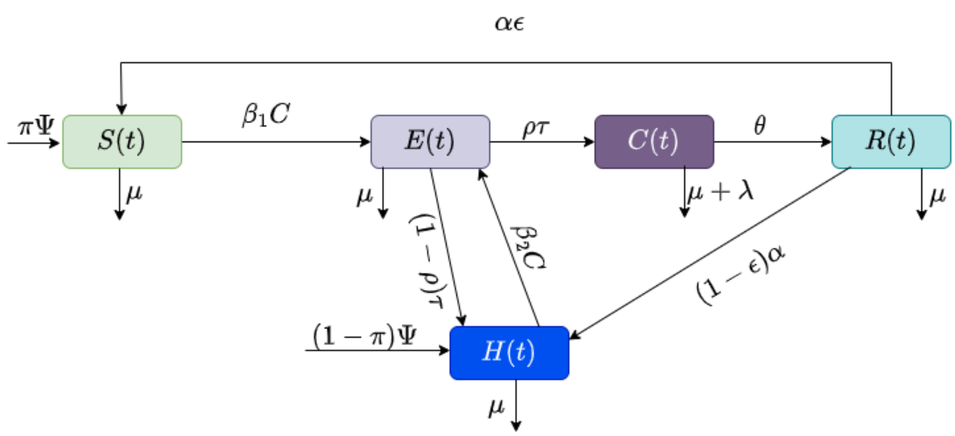


FIGURE 1. Schematic diagram depicting the transmission dynamics of model

$$
\begin{aligned}
\frac{dS(t)}{dt} &= \pi\Psi - \beta_1 C(t)S(t) + \alpha\epsilon R(t) - \mu S(t),\\
\frac{dE(t)}{dt} &= (\beta_1 S(t) + \beta_2 H(t))C(t) - (\tau+\mu)E(t),\\
\frac{dC(t)}{dt} &= \rho\tau E(t) - (\lambda+\theta+\mu)C(t),\\
\frac{dR(t)}{dt} &= \theta C(t) - (\alpha+\mu)R(t),\\
\frac{dH(t)}{dt} &= (1-\pi)\Psi + (1-\rho)\tau E(t) + (1-\epsilon)\alpha R(t) - \beta_2 C(t)H(t) - \mu H(t),
\end{aligned}
\tag{1}
$$

with initial conditions

$$S(0) = S_0, E(0) = E_0, C(0) = C_0, R(0) = R_0, H(0) = H_0$$

where

$$N(t) = S(t) + E(t) + C(t) + R(t) + H(t).$$

| *Variables & Parameters* | *Description* |
|---|---|
| $S(t)$ | Susceptible |
| $E(t)$ | Exposed individual |
| $C(t)$ | Corrupt individual |
| $R(t)$ | Recovered individual |
| $H(t)$ | Honest individual |
| $\Psi$ | Recruitment rate of susceptible and honest individuals |
| $\pi$ | proportion of recruitment that susceptible |
| $\beta_1$ | Contact rate of corrupted human with susceptible |
| $\beta_2$ | Contact rate of corrupted human with honest individuals |
| $\epsilon$ | Proportion of recovered that becomes susceptible |
| $\alpha$ | Conversion rate of recovered to honest or susceptible |
| $\tau$ | Rate of exposed showing honesty or becoming corrupt |
| $\rho$ | Proportion of exposed that becomes corrupt |
| $\theta$ | Conversion rate of corrupt to recover |
| $\mu$ | Natural death rate |
| $\lambda$ | Rate of imprisonment due to corruption |

TABLE 1. Description of variables and parameters

## 3. The Model basic properties

### 3.1. **The basic reproduction number.**

$$\mathcal{F} = \begin{bmatrix} (\beta_1 S + \beta_2 H)C \\ 0 \\ 0 \\ 0 \end{bmatrix}, \quad \mathcal{V} = \begin{bmatrix} (\tau+\mu)E \\ -\rho\tau E + (\lambda+\theta+\mu)C \\ -\theta C + (\alpha+\mu)R(t) \\ -(1-\pi)\Psi - (1-\rho)\tau E - (1-\epsilon)\alpha R + \beta_2 CH + \mu H(t) \end{bmatrix}$$

Equation (1) has corrupt free equilibrium $E_0 = (\frac{\Psi}{\mu}, 0, 0, 0, \frac{(1-\pi)\Psi}{\mu})$. The Jacobian of $\mathcal{F}$ and $\mathcal{V}$ at $E_0$ are

$$F = \begin{bmatrix} 0 & \frac{\beta_2(1-\pi)\Psi}{\mu} + \frac{\beta_1\Psi}{\mu} & 0 & 0 \\ 0 & 0 & 0 & 0 \\ 0 & 0 & 0 & 0 \\ 0 & 0 & 0 & 0 \end{bmatrix} \quad V = \begin{bmatrix} \mu+\tau & 0 & 0 & 0 \\ -\rho\tau & \mu+\theta+\lambda & 0 & 0 \\ 0 & -\theta & \alpha+\mu & 0 \\ -(1-\rho)\tau & \frac{\beta_2(1-\pi)\Psi}{\mu} & -(1-\epsilon)\alpha & \mu \end{bmatrix}$$

and the inverse of $V$ is

$$V^{-1} = \begin{bmatrix} \frac{1}{\mu+\tau} & 0 & 0 & 0 \\ \frac{\rho\tau}{(\mu+\theta+\lambda)(\mu+\tau)} & \frac{1}{\mu+\theta+\lambda} & 0 & 0 \\ \frac{\theta\rho\tau}{(\mu+\theta+\lambda)(\mu+\tau)(\alpha+\mu)} & \frac{\theta}{(\mu+\theta+\lambda)(\alpha+\mu)} & \frac{1}{\alpha+\mu} & 0 \\ AA & \frac{\Psi\alpha\pi\beta_2+\Psi\mu\pi\beta_2-\alpha\theta\mu\epsilon-\Psi\alpha\beta_2-\Psi\mu\beta_2+\alpha\theta\mu}{\mu^2(\mu+\theta+\lambda)(\alpha+\mu)} & -\frac{(-1+\epsilon)\alpha}{(\alpha+\mu)\mu} & \frac{1}{\mu} \end{bmatrix},$$

where

$$AA = \frac{\tau\left(\left(\Psi\left(\pi-1\right)\left(\alpha+\mu\right)\beta_2-\mu\alpha\theta\epsilon\right)\rho-\left(\alpha+\theta+\lambda\right)\left(\rho-1\right)\mu^2-\left(\left(\left(\rho-1\right)\lambda-\theta\right)\alpha+\left(\rho-1\right)\mu^2\right)\mu\right)}{\left(\tau+\mu\right)\left(\theta+\lambda+\mu\right)\left(\alpha+\mu\right)\mu^2}.$$

$$FV^{-1} = \begin{bmatrix} \frac{\left(\frac{\beta_2(1-\pi)\Psi}{\mu}+\frac{\beta_1\Psi}{\mu}\right)\rho\tau}{(\tau+\mu)(\theta+\lambda+\mu)} & \frac{\frac{\beta_2(1-\pi)\Psi}{\mu}+\frac{\beta_1\Psi}{\mu}}{\theta+\lambda+\mu} & 0 & 0 \\ 0 & 0 & 0 & 0 \\ 0 & 0 & 0 & 0 \\ 0 & 0 & 0 & 0 \end{bmatrix}$$

The matrix, $FV^{-1}$, which is non-negative, is the next generation matrix of equations (1). The basic reproduction number that corresponds to this is

$$R_0 = \frac{\Psi\rho\tau\beta_1}{\mu\left(\mu+\theta+\lambda\right)\left(\mu+\tau\right)} - \frac{\Psi\rho\tau\beta_2\left(\pi-1\right)}{\mu\left(\mu+\theta+\lambda\right)\left(\mu+\tau\right)} \tag{2}$$

3.2. **Analysis of the Positivity and Boundedness of the Solution to the Model.** To establish the positivity and boundedness of equation (1), we employ the following theorem

*Theorem* 3.1. Taking into account each compartment, which represents the human population, let the initial value for each compartment be $\{S(t) \geq 0, \quad E(t) \geq 0, \quad C(t) \geq 0, \quad H(t) \geq 0, \quad R(t) \geq 0\} \in \Omega$, and

$$\Omega = \left\{(S(t), E(t), C(t), H(t), R(t)) \in \mathbb{R}_+^5 : 0 \leq S(t)+E(t)+C(t)+H(t)+R(t) \leq \frac{\Psi}{\mu}\right\}.$$

Therefore,the solution set $\{S(t), E(t), C(t), H(t), R(t)\}$ for model (1) is positive for all values of time $t$.

*Proof.* Let

$$q = \sup\{t > 0 : S(t) > 0, E(t) > 0, C(t) > 0, H(t) > 0, R(t) > 0\} \in [0, t]$$

When $t > 0$, the following inequality holds

$$\frac{dS(t)}{dt} = \pi\Psi - \beta_1 C(t)S(t) + \alpha\epsilon R(t) - \mu S(t) \geq \pi\Psi - (\beta_1 C(t) - \mu)S(t),$$

i.e

$$\frac{dS(t)}{dt} + (\beta_1 C(t) - \mu)S(t) \geq \pi\Psi \tag{3}$$

This is first order non-homogeneous ordinary differential equation and is not exact. Therefore, the integrating factor is given as

$$IF = e^{\mu t + \beta_1\int_0^t C(t)dt} \tag{4}$$

by applying (4) on (3), we have

$$\frac{d}{dt}\left[S(t)e^{\mu t+\beta_1\int_0^t C(n)dn}\right] \geq \pi\Psi e^{\mu t+\beta_1\int_0^t C(n)dn}$$

Solve and integrate from 0 to $q$, we obtain

$$S(q) = e^{-\{\mu q+\beta_1\int_0^q C(n)dn\}} \times \left(S(0) + \pi\Psi\int_0^q e^{\mu t+\beta_1\int_0^t C(n)dn}\right) > 0. \tag{5}$$

Because all of the state variables are positive in the range $[0,q]$, hence the value of $S(t) > 0$. Utilizing the same thought process, we can show that $E(t), C(t), H(t)$ and $R(t)$ are all greater or equal to zero. □

*Theorem* 3.2. Assume that none of the model's initial conditions have a negative value in the $\mathbb{R}^6$, all the solutions of the model (1) has an upper and lower limit if $\lim_{t\to\infty}\sup N(t) \leq \frac{\Psi}{\mu}$, then

$$N(t) = S(t) + E(t) + C(t) + H(t) + R(t)$$

*Proof.*

$$\frac{dN(t)}{dt} = \frac{dS(t)}{dt} + \frac{dE(t)}{dt} + \frac{C(t)}{dt} + \frac{dH(t)}{dt} + \frac{dR(t)}{dt}$$

$$\frac{dN(t)}{dt} = \Psi - \mu(S(t) + E(t) + C(t) + H(t) + R(t)) - \lambda C = \Psi - \mu N(t) - \lambda C(t)$$

$$\frac{dN(t)}{dt} \leq \Psi - \mu N(t) \tag{6}$$

Solving equation (6), we obtain

$$N(t) \leq \frac{\Psi}{\mu} - \left(\frac{\Psi}{\mu} - N(0)\right)e^{-\mu t} \tag{7}$$

Taking the limit of equation (7) as $t$ goes to infinity, we have

$$\lim_{t\to\infty}\sup N(t) \leq \frac{\Psi}{\mu} \tag{8}$$

Equation (8) demonstrated that the model (1) is bounded. □

3.3. **Corruption Free Equilibrium Local Asymptotic Stability.** If $R_0 < 1$, the Corruption Free Equilibrium (CFE) is locally asymptotically stable and unstable if $R_0 > 1$. To determine the local stability of the CFE, one can analyze the real parts of the eigenvalues of the Jacobiam matrix formed from the model (1) with respect to the state variables $S(t), E(t), C(t), H(t)$ and $R(t)$. If all eigenvalues are negative, then the equilibrium point is stable; otherwise, it is unstable.

Evaluate the Jocobian matrix of model (1) at corruption free equilibrium $E_0$, we obtain

$$J(E_0) = \begin{bmatrix} -\mu & 0 & -\frac{\beta_1\Psi}{\mu} & \alpha\epsilon & 0 \\ 0 & -\tau-\mu & \frac{\beta_2(1-\pi)\Psi}{\mu} + \frac{\beta_1\Psi}{\mu} & 0 & 0 \\ 0 & \rho\tau & -\lambda-\theta-\mu & 0 & 0 \\ 0 & 0 & \theta & -\alpha-\mu & 0 \\ 0 & (1-\rho)\tau & -\frac{\beta_2(1-\pi)\Psi}{\mu} & (1-\epsilon)\alpha & -\mu \end{bmatrix}$$

The eigenvalues of the matrix $J(E_0)$ are given as:

$$\lambda_1 = -(\tau + \mu), \quad \lambda_2 = -(\alpha + \mu), \quad \lambda_4 = -\mu, \quad \lambda_5 = -\mu$$

$$\lambda_3 = -\frac{(\beta_2(-1+\pi) - \beta_1)\,\rho\tau\Psi + \mu(\mu+\theta+\lambda)(\tau+\mu)}{(\tau+\mu)\,\mu}$$

Sice all the eigenvalues are negative, this indicates that the CFE is locally stable in an asymptotic sense.

3.4. **Corruption Free Equilibrium Global Stability.** Here we adopt the LaSalle's invariance principle to determine the global stability of corruption free equilibrium (CFE). Suppose $K = \frac{C^2}{2}$, therefore $\frac{dK}{dC} = C$. From second equation in model(1),we have

$$\frac{dC(t)}{dt} = \rho\tau E(t) - (\lambda + \theta + \mu)C(t)$$

Using chain's rule

$$\begin{aligned}\frac{dK}{dt} &= \frac{dK}{dC} \times \frac{dC}{dt} \\ &= C\Big(\rho\tau E(t) - (\lambda+\theta+\mu)C\Big) \\ &= C^2\Big(\frac{\rho\tau(\beta_1 S(t) + \beta_2 H(t))}{\tau+\mu} - (\lambda+\theta+\mu)\Big),\end{aligned}$$

using E(t) at corrupt free equilibrium and the basic reproduction number, we have $\tau + \mu = \frac{\Psi\rho\tau(\beta_1 - \beta_2(\pi-1))}{R_0\mu(\lambda+\theta+\mu)}$

$$\frac{dK}{dt} = C^2(\lambda+\theta+\mu)\left[\frac{\mu(\beta_1 S(t) + \beta_2 H(t))}{\beta_1 - \beta_2(\pi-1)} R_0 - 1\right]$$

but $\frac{\mu(\beta_1 S(t)+\beta_2 H(t))}{\beta_1 - \beta_2(\pi-1)} < 1$ This implies that

$$\frac{dK}{dt} \leq C^2(\lambda+\theta+\mu)\Big[R_0 - 1\Big]$$

Therefore

$$\frac{dK}{dt} \leq C^2(\lambda+\theta+\mu)\Big[R_0 - 1\Big] \leq 0 \quad \text{if} \quad R_0 \leq 1 \tag{9}$$

The corruption free equilibrium (CFE) is globally stable for $R_0 < 1$ in this situation.

3.5. **Analytical interpretation and sensitivity analysis of the Basic Reproduction Number.** Sensitivity is the process of evaluating the impact of individual parameters on the basic reproduction number. This is done to determine the extent to which each parameter influences the value of the basic reproduction number. This approach is useful when selecting a corruption control strategy that addresses the most significant factors in a sensitive manner. In this context, we calculate the sensitivity indices for the basic reproduction number, $R_0$.

**Proposition 3.1.** *An increase in both parameters $\Psi, \rho, \tau, \beta_1$ and $\beta_2$ leads to an increase in the basic reproduction number.*

*Proof.*

$$\frac{\partial R_0}{\partial \Psi}=\frac{\rho\tau\left(\beta_1-\beta_2\left(\pi-1\right)\right)}{\mu\left(\theta+\lambda+\mu\right)\left(\tau+\mu\right)}>0,\quad \frac{\partial R_0}{\partial \rho}=\frac{\Psi\tau\left(\beta_1-\beta_2\left(\pi-1\right)\right)}{\mu\left(\theta+\lambda+\mu\right)\left(\tau+\mu\right)}>0$$

$$\frac{\partial R_0}{\partial \tau}>0,\frac{\partial R_0}{\partial \beta_1}=\frac{\Psi\rho\tau}{\mu\left(\theta+\lambda+\mu\right)\left(\tau+\mu\right)}>0,\quad \frac{\partial R_0}{\partial \beta_2}=\frac{\Psi\rho\tau\left(-\pi+1\right)}{\mu\left(\theta+\lambda+\mu\right)\left(\tau+\mu\right)}>0$$

□

**Proposition 3.2.** *An increase in both parameters $\theta, \lambda, \pi$ and $\mu$ leads to an decrease in the basic reproduction number.*

*Proof.*

$$\frac{\partial R_0}{\partial \theta}=-\frac{\Psi\rho\tau\left(\beta_1-\beta_2\left(\pi-1\right)\right)}{\mu\left(\theta+\lambda+\mu\right)^2\left(\tau+\mu\right)}<0,\quad \frac{\partial R_0}{\partial \lambda}=-\frac{\Psi\rho\tau\left(\beta_1-\beta_2\left(\pi-1\right)\right)}{\mu\left(\theta+\lambda+\mu\right)^2\left(\tau+\mu\right)}<0$$

$$\frac{\partial R_0}{\partial \pi}=-\frac{\Psi\rho\tau\beta_2}{\mu\left(\theta+\lambda+\mu\right)\left(\tau+\mu\right)}<0,\quad \frac{\partial R_0}{\partial \mu}<0$$

□

Utilising [19]- [20], we define the normalized forward sensitivity index of a variable, $\mathbb{L}$, that depends differentiably on a parameter, $\omega$ is defined as

$$Z_{\omega}^{\mathbb{L}}=\frac{\partial \mathbb{L}}{\partial \omega}\times\frac{\omega}{|\mathbb{L}|}$$

A positive normalized forward sensitivity index indicates that an increase in the corresponding independent variable will lead to an increase in the dependent variable, while a negative normalized forward sensitivity index indicates that an increase in the independent variable will lead to a decrease in the dependent variable. The magnitude of the normalized forward sensitivity index can also provide information on the sensitivity of the dependent variable to changes in the independent variable. A larger magnitude of normalized forward sensitivity index indicates a stronger influence of the independent variable on the dependent variable.

The sensitivity indices of $R_0$ to the model's parameters are evaluated at the parameter baseline and are displayed in the table below.

The sensitivity index table reveals that $\Psi$ and $\rho$ are the parameters that exert the most significant influence on the outcome of the analysis. Based on the value of $Z_{\omega}^{\mathbb{L}}=+1$ for both $\Psi$ and $\rho$, a 10% decrease in $\Psi$ and $\rho$ will lead to a 10% reduction in $R_0$ respectively, while a 10% increase in $\Psi$ and $\rho$ will correspondingly result in a 10% increase in $R_0$ respectively.

In Figure 2, the normalized forward sensitivity indices for the basic reproduction number are showcased, highlighting how each of the baseline parameter values impact the basic reproduction number.

| S/N | Parameter | Sensitivity index | Comment |
|---|---|---|---|
| 1 | $\Psi$ | $+1$ | Enhanced the spread of corruption |
| 2 | $\tau$ | $+0.0211132$ | Enhanced the spread of corruption |
| 3 | $\beta_1$ | $+0.7250982$ | Enhanced the spread of corruption |
| 4 | $\beta_2$ | $+0.2749018$ | Enhanced the spread of corruption |
| 5 | $\pi$ | $-0.0921233$ | Eradicate the spread of corruption |
| 6 | $\mu$ | $-1.0559212$ | Eradicate the spread of corruption |
| 7 | $\theta$ | $-0.9651303$ | Eradicate the spread of corruption |
| 8 | $\lambda$ | $-0.0000617$ | Eradicate the spread of corruption |
| 9 | $\rho$ | $+1$ | Enhanced the spread of corruption |

Table 2. Sensitivity index.

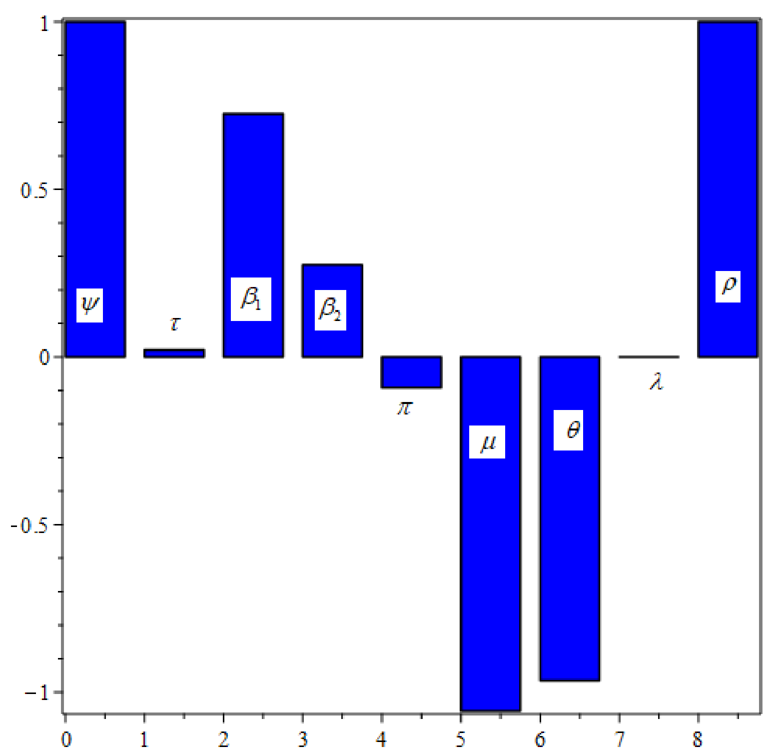


Figure 2. Sensitivity indices graph

3.6. **Bifurcation of dynamical system.** Here, we utilize the bifurcation analysis method developed by [21] to analyze the model (1). Specifying

$$S(t) = x_1, \quad E(t) = x_2 \quad C(t) = x_3 \quad R(t) = x_4 \quad H(t) = x_5$$

The model (q1) undergoes a transformation and becomes

$$\begin{aligned}
\frac{dx_1}{dt} &= \pi\Psi - \beta_1 x_1 x_3 + \alpha\epsilon x_4 - \mu x_1 := f_1, \\
\frac{dx_2}{dt} &= (\beta_1 x_1 + \beta_2 x_5)x_3 - (\tau + \mu)x_2 := f_2, \\
\frac{dx_3}{dt} &= \rho\tau x_2 - (\lambda + \theta + \mu)x_3 := f_3, \\
\frac{dx_4}{dt} &= \theta x_3 - (\alpha + \mu)x_4 := f_4, \\
\frac{dx_5}{dt} &= (1-\pi)\Psi + (1-\rho)\tau x_2 + (1-\epsilon)\alpha x_4 - \beta_2 x_3 x_5 - \mu x_5 := f_5,
\end{aligned} \tag{10}$$

Given that the value of the bifurcation parameter is assumed to be $\tau$, the fact that $R_0 = 1$ inevitably leads to the conclusion that

$$\tau = -\frac{\mu^2(\theta + \lambda + \mu)}{\pi\Psi\rho\beta_2 - \Psi\rho\beta_1 - \Psi\rho\beta_2 + \lambda\mu + \mu^2 + \theta\mu} := \tau * .$$

We describe the system of ordinary differential equations as

$$x'(t) = f(x, \tau *)$$

such that the function $f$ is $f : \mathbb{R}^n \times \mathbb{R} \to \mathbb{R}^n$ and is of $\mathbb{C}^n$. The system of differential equations described earlier is assumed to have an equilibrium point at zero for all parameter values $\tau*$, i.e $f(0, \tau*) = 0, \forall \tau*$ The eigenvalues of the characteristic polynomial of the equatin (10), $J(E_0, \tau*)$ are written as

$$\lambda_1 = -(\tau + \mu), \quad \lambda_2 = -(\alpha + \mu), \quad \lambda_4 = -\mu, \quad \lambda_5 = -\mu \quad \lambda_3 = 0$$

Hence, the matrix $J(E_0, \tau^*)$, has a simple zero eigenvalue at $\lambda_3 = 0$ while the remaining eigenvalues are real and negative.

$\mathbf{w} = (w_1, w_2, w_3, w_4, w_5)^T$ denotes the right eigenvector corresponding to the zero eigenvalue $\lambda_3 = 0$. It is obtained by the following procedure:

$$\begin{bmatrix}
-\mu & 0 & -\frac{\beta_1\Psi}{\mu} & \alpha\epsilon & 0 \\
0 & -(\tau^* + \mu) & \frac{\beta_2\Psi(1-\pi)}{\mu} + \frac{\beta_1\Psi}{\mu} & 0 & 0 \\
0 & \rho\tau^* & -(\lambda + \theta + \mu) & 0 & 0 \\
0 & 0 & \theta & -(\alpha + \mu) & 0 \\
0 & (1-\rho)\tau^* & -\frac{\beta_2\Psi(1-\pi)}{\mu} & \alpha(1-\epsilon) & -\mu
\end{bmatrix}
\begin{bmatrix} w_1 \\ w_2 \\ w_3 \\ w_4 \\ w_5 \end{bmatrix}
=
\begin{bmatrix} 0 \\ 0 \\ 0 \\ 0 \\ 0 \end{bmatrix}$$

Hence

$$w_1 = \frac{\rho\overline{\tau}\left(\left(\pi - 1\right)\beta_2 - \beta_1\right)\left(\alpha + \mu\right)\Psi + \alpha\epsilon\theta\mu}{\mu^2\left(\alpha + \mu\right)} \quad w_2 = \theta + \lambda + \mu, \quad w_3 = \rho\tau^*$$

$$w_4 = \frac{\theta\rho\tau^*}{\alpha+\mu}, \quad w_5 = \frac{\tau^*(L\rho - \mu\left(\mu^2 + (\alpha+\theta+\lambda)\mu + \alpha\lambda\right)\rho + \mu(\lambda+\theta+\mu)(\alpha+\mu))}{\mu^2(\alpha+\mu)}$$

where

$$L = \Psi(\pi-1)(\alpha+\mu)\beta_2 - \alpha\epsilon\theta\mu$$

As a result, the right eigenvectors is $\mathbf{w} = (w_1, w_2, w_3, w_4, w_5)^T$. Furthermore, the left eigenvector must fulfill the condition $\mathbf{v}\cdot\mathbf{w} = 1$, which can be expressed as $\mathbf{v} = (v_1, v_2, v_3, v_4, v_5, v_6)$ is given by

$$\begin{bmatrix} v_1, v_2, v_3, v_4, v_5 \end{bmatrix} \begin{bmatrix} -\mu & 0 & -\frac{\beta_1\Psi}{\mu} & \alpha\epsilon & 0 \\ 0 & -(\tau^*+\mu) & \frac{\beta_2\Psi(1-\pi)}{\mu} + \frac{\beta_1\Psi}{\mu} & 0 & 0 \\ 0 & \rho\tau^* & -(\lambda+\theta+\mu) & 0 & 0 \\ 0 & 0 & \theta & -(\alpha+\mu) & 0 \\ 0 & (1-\rho)\tau^* & -\frac{\beta_2\Psi(1-\pi)}{\mu} & \alpha(1-\epsilon) & -\mu \end{bmatrix} = \begin{bmatrix} 0 \\ 0 \\ 0 \\ 0 \\ 0 \end{bmatrix}$$

$$\begin{cases} -\mu v_1 = 0 \\ -(\tau^*+\mu)v_2 + \rho\tau^* v_3 + (1-\rho)\tau^* v_4 = 0 \\ -\frac{\beta_1\Psi}{\mu}v_1 + \left(\frac{\beta_2\Psi(1-\pi)}{\mu} + \frac{\beta_1\Psi}{\mu}\right)v_2 - (\lambda+\theta+\mu)v_3 + \theta v_4 - \frac{\beta_2\Psi(1-\pi)}{\mu}v_5 = 0 \\ \alpha\epsilon v_1 - (\alpha+\mu)v_4 + \alpha(1-\epsilon)v_5 v_5 = 0 \\ -\mu v_5 = 0 \end{cases}$$

By solving these equations, we can have

$$v_1 = v_4 = v_5 = 0, \quad v_2 = \frac{1}{\lambda+2\mu+\tau^*+\theta}, \quad v_3 = \frac{\tau^*+\mu}{\rho\tau^*(\lambda+2\mu+\tau^*+\theta)}$$

Upon estimating second order partial derivatives at the corrup-free-equilibrium of equation (10), we obtain the following:

$$\frac{\partial^2 f_1}{\partial x_1 \partial x_3} = \frac{\partial^2 f_1}{\partial x_3 \partial x_1} = -\beta_1, \frac{\partial^2 f_2}{\partial x_1 \partial x_3} = \frac{\partial^2 f_2}{\partial x_3 \partial x_1} = \beta_1, \frac{\partial^2 f_2}{\partial x_3 \partial x_5} = \frac{\partial^2 f_2}{\partial x_5 \partial x_3} = \beta_2,$$

$$\frac{\partial^2 f_5}{\partial x_3 \partial x_5} = \frac{\partial^2 f_5}{\partial x_5 \partial x_3} = -\beta_2, \frac{\partial^2 f_2}{\partial x_2 \partial \tau} = \frac{\partial^2 f_2}{\partial \tau \partial x_2} = -1, \frac{\partial^2 f_3}{\partial x_2 \partial \tau} = \frac{\partial^2 f_3}{\partial \tau \partial x_2} = \rho$$

and

$$\frac{\partial^2 f_5}{\partial x_2 \partial \tau} = \frac{\partial^2 f_5}{\partial \tau \partial x_2} = (1-\rho).$$

On the other hand, the values of all of the other second-order derivatives return back to zero.

To determine the coefficients of $\mathbf{a}$ and $\mathbf{b}$ in accordance with [21], we assume that $f_q$ represents the $qth$ component of $f$ and then proceed as follows:

$$\mathbf{a} = \sum_{q,i,j=1}^{5} v_q w_i w_j \frac{\partial^2 f_q}{\partial x_i \partial x_j}(E_0, \tau^*) \tag{12}$$

$$\mathbf{b} = \sum_{q,i,j=1}^{5} v_q w_i \frac{\partial^2 f_q}{\partial x_i \partial \tau}(E_0, \tau^*) \tag{13}$$

The values of coefficients **a** and **b** hold significant importance in determining the local behavior of equation (1) at the point where x equals zero. These are evaluated and completely determined. Taking into consideration the equation (10) in the estimation of the coefficients of **a** and **b**, the derivatives of the second order that are not zero for the terms for the terms $\frac{\partial^2 f_q}{\partial x_i \partial x_j}(E_0, \tau)$ and $\frac{\partial^2 f_q}{\partial x_i \partial \tau}(E_0, \tau)$ are given as follows:

$$\begin{aligned}\mathbf{a} &= 2v_1 w_1 w_3 \frac{\partial^2 f_1}{\partial x_1 \partial x_3}(E_0, \tau^*) + 2v_2 w_1 w_3 \frac{\partial^2 f_2}{\partial x_1 \partial x_3}(E_0, \tau^*) \\ &+ 2v_2 w_3 w_5 \frac{\partial^2 f_2}{\partial x_3 \partial x_5}(E_0, \tau^*) + 2v_5 w_3 w_5 \frac{\partial^2 f_5}{\partial x_3 \partial x_5}(E_0, \tau^*)\end{aligned}$$

and

$$\mathbf{b} = v_2 w_2 \frac{\partial^2 f_2}{\partial x_2 \partial \tau}(E_0, \tau^*) + v_3 w_2 \frac{\partial^2 f_3}{\partial x_2 \partial \tau}(E_0, \tau^*) + v_5 w_2 \frac{\partial^2 f_5}{\partial x_2 \partial \tau}(E_0, \tau^*)$$

This implies

$$\mathbf{a} = 2v_2 w_1 w_3 \beta_1 + 2v_2 w_3 w_5 \beta_2$$

and

$$\mathbf{b} = -v_2 w_2 + v_3 w_2 \rho$$

$$\begin{aligned}\mathbf{a} = &\frac{2\left(\rho\tau\left((\pi-1)\beta_2 - \beta_1\right)(\alpha+\mu)\Psi + \alpha\epsilon\theta\mu\right)\rho\tau\beta_1}{(\lambda+2\mu+\tau+\theta)\mu^2(\alpha+\mu)} \\ &+ \frac{2\rho\tau^2\left(n_1\rho - \mu\left(\mu^2 + (\alpha+\theta+\lambda)\mu + \alpha\lambda\right)\rho + \mu(\lambda+\theta+\mu)(\alpha+\mu)\right)\beta_2}{(\lambda+2\mu+\tau+\theta)\mu^2(\alpha+\mu)} > 0\end{aligned}$$

where

$$n_1 = \Psi(\pi-1)(\alpha+\mu)\beta_2 - \alpha\epsilon\theta\mu$$

$$\mathbf{b} = \frac{(\theta+\lambda+\mu)\mu}{\tau(\lambda+2\mu+\tau+\theta)} > 0$$

We have found that both the coefficients **a** and **b** have values that are strictly larger than zero. In other words, neither **a** nor **b** can be zero or negative in the context of the situation being discussed. Follow [21], since both **a** and **b** are positive, the behavior of the equilibrium point depends on the value of the parameter $\tau^*$.

When $\tau^*$ is negative and its absolute value is very small, then the equilibrium point $x = 0$ is locally asymptotically stable, meaning that nearby solutions to the differential equation approach $x = 0$ over time. Additionally, there is a positive unstable equilibrium point, indicating that there is another equilibrium point towards which nearby solutions move away over time.

On the other hand, when $\tau^*$ is positive, the equilibrium point $x = 0$ is unstable, meaning that nearby solutions move away from $x = 0$ over time. Instead, there exists a negative locally asymptotically stable equilibrium point, indicating that there is another equilibrium point towards which nearby solutions approach over time.

| Parameter | Values | Sources |
|---|---|---|
| $\Psi$ | 0.026 | Asummed |
| $\beta_2 1$ | 0.081, 0.31,0.51 | Varied |
| $\beta_2$ | 0.041, 0.31,0.51 | Varied |
| $\epsilon$ | 0.077 | Assumed |
| $\alpha$ | 0.072 | Assumed |
| $\tau$ | 0.510 | Assumed |
| $\rho$ | 0.67,0.77,0.97 | Varied |
| $\theta$ | 0.305,0.5,0.7 | Varied |
| $\mu$ | 0.011 | [5] |
| $\lambda$ | $0.195 \times 10^{-4}$,0.05,0.1 | Varied |
| $\pi$ | 0.251 | Assumed |

TABLE 3. Estimated model parameters [5], [22]- [23]

## 4. Numerical Simulation and Results

To ensure the completion of the analytical study, it is crucial to validate the data through numerical simulation. In this section, we have included various numerical simulations to track the dynamics of system (1) under different initial compartmental variable of susceptible individuals, exposed individuals, corrupted individuals, recovered individuals, and honest individual as $S(0) = 0.4, E(0) = 0.3, C(0) = 0.2.R(0) = 0$ and $H(0) = 01$ respectively together with specified parameters given in Table 3.

The overall dynamics of the compartmental models are presented in Figure 3. The number of susceptible individuals decreases at the beginning, and then gradually starts to increase after a few years. Meanwhile, the number of exposed individuals decreases until it reaches zero, while the number of corrupted individuals initially increases and then starts to decline after a few years. The number of recovered individuals increases until it reaches its peak after 10 years and then begins to decline. Additionally, the number of honest individuals increases rapidly for the first four years, after which the rate of increase slows down.

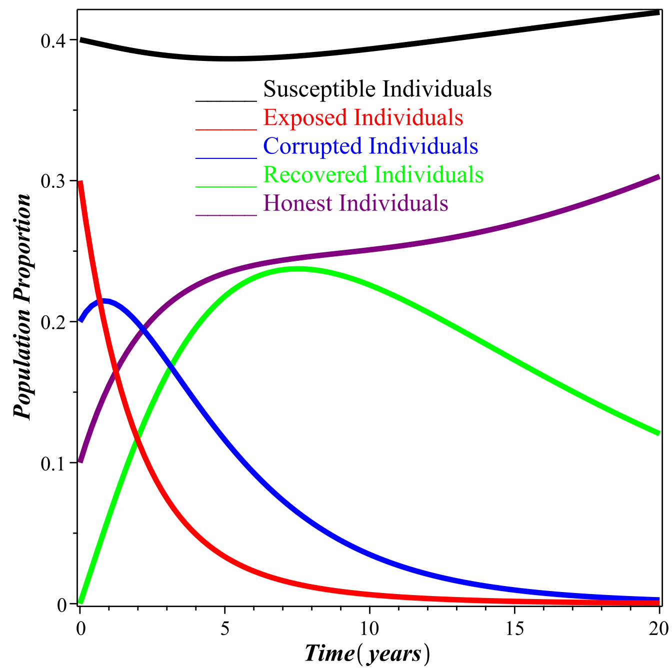


FIGURE 3. Behaviour of total population

The effects of $\lambda, \rho, \theta.\beta_1$ and $\beta_2$ on the corrupted individuals are shown in Figs [4-8]. It is noted in fig.4 that as $\lambda$ is increasing, the number of corrupted individuals decreases. This implies that more corrupt individuals are being punished and sent to prison, which act as a deterrent to others who may be considering engaging in corrupt activities, as they may fear facing the same consequences if caught. Figure 5 depicts as the $\rho$is increasing, the number of corrupt individuals surges. This shows that more people are giving in to corruption. Because of this, the number of corrupted people in society would go up. This could lead to a cycle of corruption where the more people get corrupted, the easier it is for others to justify doing corrupt things, which leads to even more corruption.

Figure 6 illustrates that increasing $\theta$ lead to decrease in the corrupt individuals populaton. As the rate of corrupted individuals turning into recovered individuals goes up, this means that more people are recovering from corruption. Because of this, the number of corrupted people in society would go down. This could start a positive cycle in which the more people who get out of corruption, the more others are encouraged to do the same, which would lead to less corruption overall. The effects of increasing $\beta_1$ and $\beta_2$ are shown in figures 7 and 8. When corrupted individuals come into contact with susceptible/honest individuals, there is a risk that the corrupt behavior will spread from the corrupted to the susceptible/honesty individuals. This can occur through various means that influence the susceptible/honest individual to engage in similar practices. As the number of corrupted individuals increases through these contacts, it becomes more likely that even more susceptible/honest individuals will be influenced and become corrupted themselves. Over time, this can lead to a widespread culture of corruption within a society, which can have detrimental effects on social and economic development.

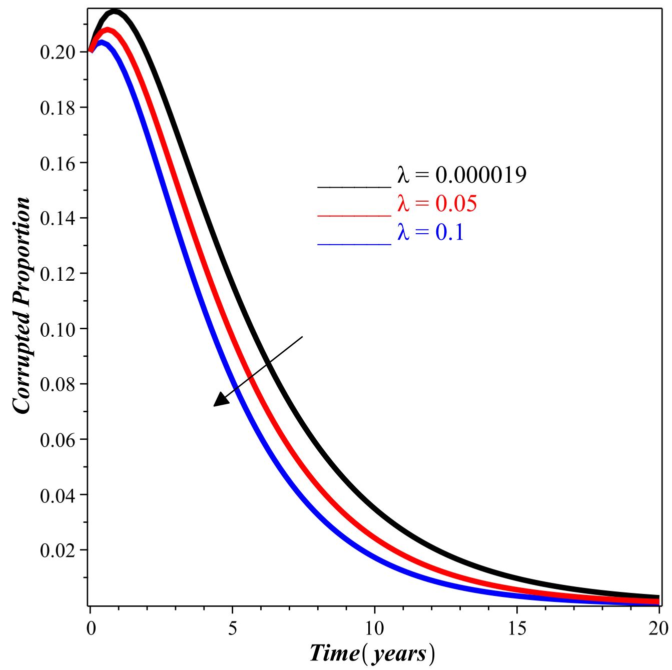


FIGURE 4. Behaviour of corrupted individual as $\lambda$ increases

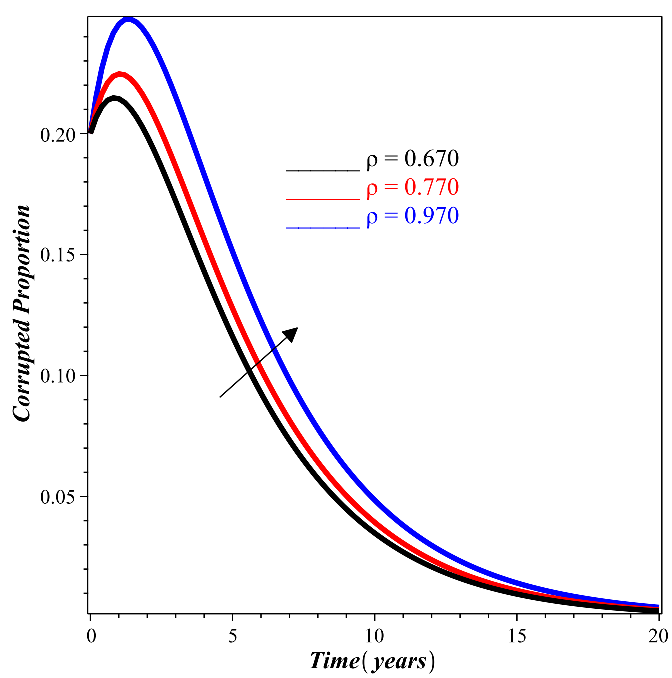


FIGURE 5. Behaviour of corrupted individual as $\rho$ increases

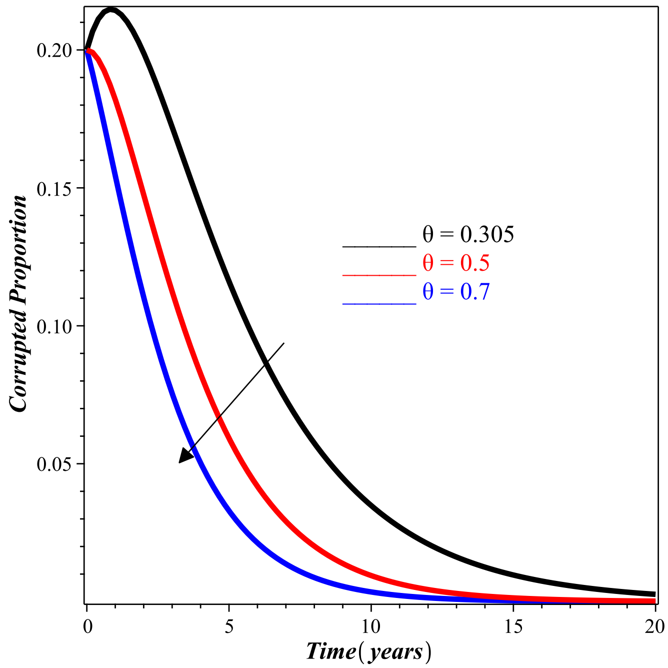


FIGURE 6. Behaviour of corrupted individual as $\theta$ increases

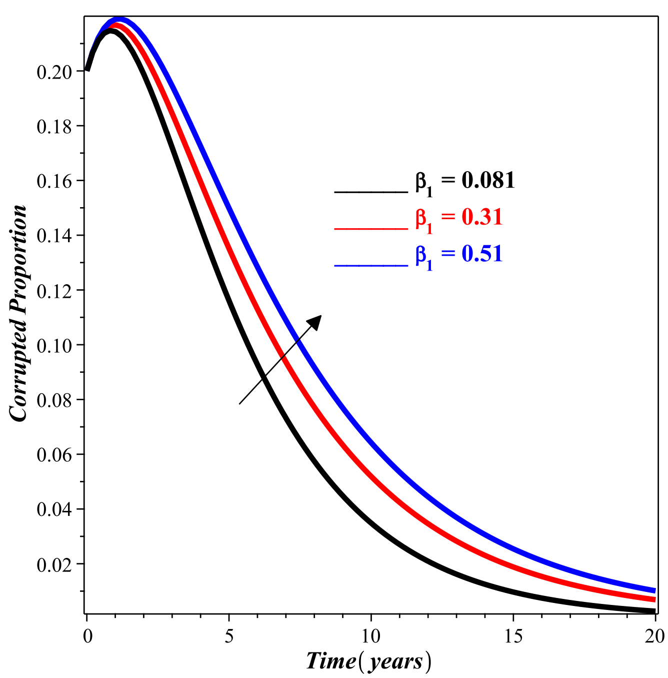


FIGURE 7. Behaviour of corrupted individual as $\beta_1$ increases

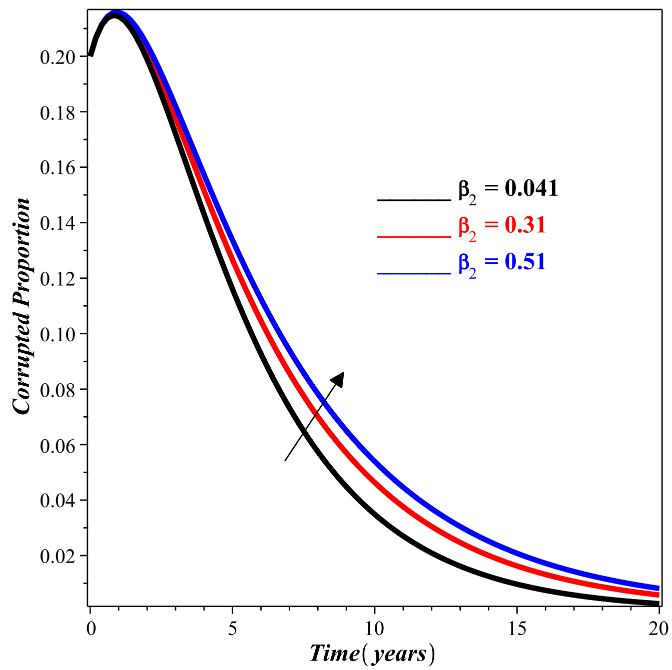


FIGURE 8. Behaviour of corrupted individual as $\beta_2$ increases

The effects of $\lambda$, $\rho$ and $\beta_1$ on the honest individuals are illustrated in figures [9-11]. Fig. 9 presents the influence of increasing $\lambda$ on the honest individuals. Increasing rate of imprisonment serves as a deterrent for individuals who might be tempted to engage in corrupt practices. When individuals witness the consequences that corrupt behavior can have on their lives and the lives of others, they may be more inclined to choose honest behavior instead, thereby increasing honest individuals population. As $rho$ is increasing, the number of honest individuals decline as shown in Fig.10. This may be attributed to the corruption can spread and harm a society's ethical standards. It fosters dishonesty and encourages unethical behavior, making it difficult for honest individuals to behave ethically. The prevalence of corruption can cause honest individuals to feel discouraged, leading to an increase in corrupt individuals and a decrease in honest individuals. This trend can continue until corruption dominates the population, leading to a decline in honest population. The effect of $\beta_2$ on honest individuals population is presented in Fig.11. An increase in $\beta_2$ decrases the population of honest individuals. When an honest individual interacts with a corrupt individual, there is a risk that the corrupt individual's behavior and values will influence the honest individual. This is especially true if the corrupt individual has a position of power or influence over the honest individual. Over time, repeated contact between corrupt individuals and honest individuals can erode the ethical values and standards of the latter. The honest individuals may become desensitized to corruption, or they may feel pressured to conform to the norms of the corrupt individuals in order to avoid negative consequences. This can lead to a decline in the number of honest individuals in the population as a whole

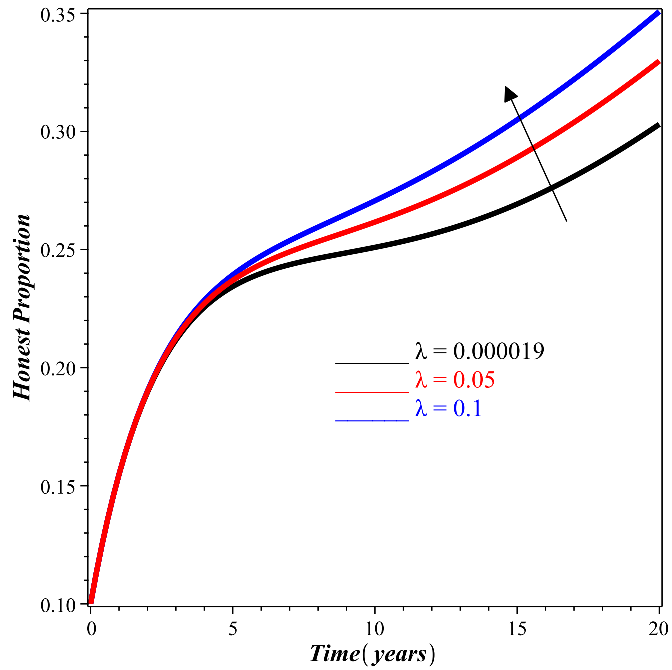


FIGURE 9. Behaviour of honest individual as $\lambda$ increases

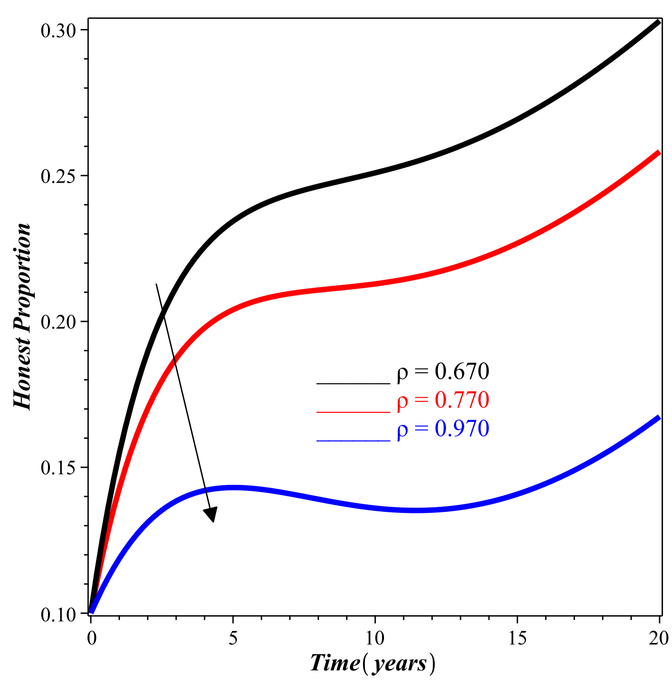


FIGURE 10. Behaviour of honest individual as $\rho$ increases

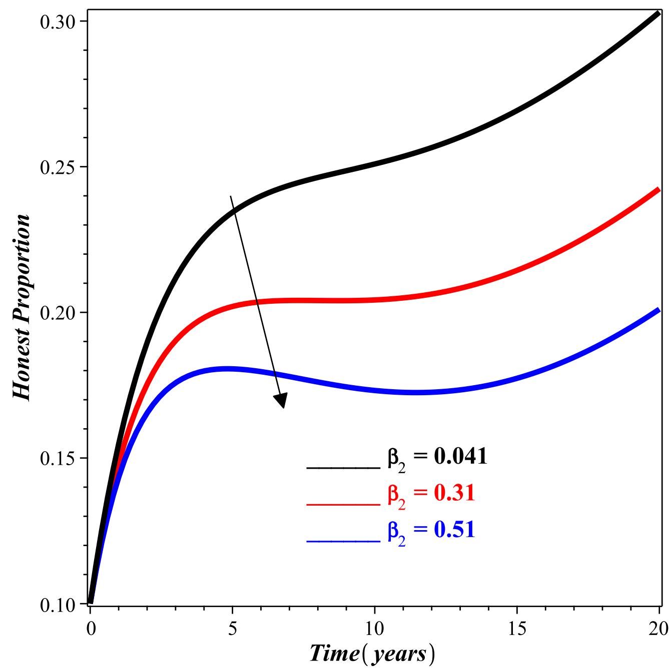


Figure 11. Behaviour of honest individual as $\beta_2$ increases

## 5. Conclusion

This paper presents a compartmental mathematical model that examines the dynamics of corruption. The model was analyzed to determine the local and global stability of the corruption-free equilibrium, and the basic reproduction number was calculated using the next generation operator method. The analysis showed that the corruption-free equilibrium is locally asymptotically stable for $R_0 < 1$. Additionally, sensitivity and bifurcation analyses were conducted, and numerical simulations were used to demonstrate the impact of parameters on the corrupt and honest compartments. The results of our simulation indicate that:

(1) An increase in the rate of imprisonment due to corruption leads to a reduction in overall corruption and promotes greater numbers of honest individuals within the population.
(2) To facilitate an increase in the number of honest individuals, it is crucial to significantly decrease the proportion of exposed individuals who become corrupted.
(3) Additionally, in order to limit the spread of corruption, it is necessary to minimize, or even eliminate, contact between corrupted and honest individuals.

## References

[1] P. Samui, J. Mondal, S. Khajanchi, A mathematical model for COVID-19 transmission dynamics with a case study of India, Chaos Solitons Fractals. 140 (2020), 110173. https://doi.org/10.1016/j.chaos.2020.110173.

[2] A.S. Eegunjobi, O.D. Makinde, Mathematical analysis of two strains of Covid-19 using SEIR model, J. Math. Fund. Sci. 54 (2022), 211-232.

[3] C) G.T. Tilahun, O.D. Makinde, D. Malonza, Modelling and optimal control of pneumonia disease with cost-effective strategies, J. Biol. Dyn. 11 (2017), 400-426. https://doi.org/10.1080/17513758.2017.1337245.

[4] A.S. Eegunjobi, M.C. Anyanwu, S.N. Neossi-Nguetchue, Modelling the super-infection of two strains of dengue virus, J. Egypt. Math. Soc. 31 (2023), 1. https://doi.org/10.1186/s42787-023-00161-6.

[5] L. Lemecha, S. Feyissa, Mathematical modeling and analysis of corruption dynamics, Ethiopian J. Sci. Sustain. Develop. 5 (2018), 13-25.

[6] Z.K. Birhanu, A.K. Fantaye, Modeling and analysis of corruption dynamics incorporating media coverage, Commun. Math. Biol. Neurosci. 2022 (2022), 94. https://doi.org/10.28919/cmbn/7651.

[7] H.T. Alemneh, Mathematical modeling, analysis, and optimal control of corruption dynamics, J. Appl. Math. 2020 (2020), 5109841. https://doi.org/10.1155/2020/5109841.

[8] N.O. Mokaya, H.T. Alemmeh, C.G. Ngari, G.G. Muthuri, Mathematical modelling and analysis of corruption of morals amongst adolescents with control measures in Kenya, Discr. Dyn. Nat. Soc. 2021 (2021), 6662185. https://doi.org/10.1155/2021/6662185.

[9] L.F. Richardson, Mathematical psychology of war, Nature. 135 (1935), 830-831. https://doi.org/10.1038/135830c0.

[10] A.W. Tesfaye, H.T. Alemneh, Analysis of a stochastic model of corruption transmission dynamics with temporary immunity, Heliyon. 9 (2023), e12752. https://doi.org/10.1016/j.heliyon.2022.e12752.

[11] O. Danford, M. Kimathi, S. Mirau, Mathematical modelling and analysis of corruption dynamics with control measures in Tanzania, J. Math. Inform. 19 (2020), 57-79.

[12] R.I. Gweryina, M.Y. Kura, E. Okwu, An epidemiological model of corruption with immunity clause in Nigeria, World J. Model. Simul. 15 (2019), 262–275.

[13] S. Athithan, M. Ghosh, X.Z. Li, Mathematical modeling and optimal control of corruption dynamics, Asian-Eur. J. Math. 11 (2018), 1850090. https://doi.org/10.1142/s1793557118500900.

[14] S. Abdulrahman, Stability analysis of the transmission dynamics and control of corruption, Pac. J. Sci. Technol. 15 (2014), 99-113.

[15] S.R. Waykar, Mathematical modelling: A comparatively mathematical study model base between corruption and development, IOSR J. Math. 6 (2013), 54-62.

[16] F.Y. Egudam, F. Oguntolu, T. Ashezua, Understanding the dynamics of corruption using mathematical modeling approach, Int. J. Innov. Sci. Eng. Technol. 4 (2017), 190-197.

[17] L. Lemecha, Modelling corruption dynamics and its analysis, Ethiopian J. Sci. Sustain. Develop. 5 (2018), 13-27.

[18] S. Athithan, M. Ghosh, X.Z. Li, Mathematical modeling and optimal control of corruption dynamics, Asian-European J. Math. 11 (2018), 1850090. https://doi.org/10.1142/s1793557118500900.

[19] N. Chitnis, J.M. Hyman, J.M. Cushing, Determining important parameters in the spread of malaria through the sensitivity analysis of a mathematical model, Bull. Math. Biol. 70 (2008), 1272-1296. https://doi.org/10.1007/s11538-008-9299-0.

[20] H.W. Berhe, O.D. Makinde, D.M. Theuri, Parameter estimation and sensitivity analysis of dysentery diarrhea epidemic model, J. Appl. Math. 2019 (2019), 8465747. https://doi.org/10.1155/2019/8465747.

[21] C. Castillo-Chavez, B. Song, Dynamical models of tuberculosis and their applications, Math. Biosci. Eng. 1 (2004), 361-404.

[22] N.O. Mokaya, H.T. Alemmeh, C.G. Ngari, G.G. Muthuri, Mathematical modelling and analysis of corruption of morals amongst adolescents with control measures in Kenya, Discr. Dyn. Nat. Soc. 2021 (2021), 6662185. https://doi.org/10.1155/2021/6662185.

[23] A.K. Fantaye, Z.K. Birhanu, Mathematical model and analysis of corruption dynamics with optimal control, J. Appl. Math. 2022 (2022), 8073877. https://doi.org/10.1155/2022/8073877.